physica status solidi b
www.pss-b.com

Effect of the Local Environment on the Magnetic Properties of Mn_3Si: Hybrid Ab Initio and Model Study

Oksana N. Draganyuk, Vyacheslav S. Zhandun, and Natalia G. Zamkova*

The effect of the local environment on the formation of magnetic moments on Mn atoms in manganese silicide Mn_3Si is studied by the combination of ab initio calculations and the model analysis. The suggested approach is related to the self-consistent mapping of the results of ab initio calculations to a multiorbital model. The model analysis allows to reveal the role played by the local environment of the transition metal atoms on the magnetic moments formation. It is found that the formation of the magnetic moment is controlled rather by hopping parameters between Mn atoms, not by the number of Mn–Si nearest neighbors. Particularly, the formation of magnetic moment on MnI atom is mainly controlled by the hopping parameter between nearest Mn atoms, while the magnetic moment on MnII atom is primarily determined by the hoppings between next-nearest Mn atoms. The obtained phase diagrams of the magnetic state show the presence of a sharp boundary with respect to the hopping between Mn atoms. This opens the opportunity to turn on or turn off the magnetic state by the external impacts. The ab initio calculations of Mn_3Si well agree with the results of model consideration and confirm the model conclusions.

1. Introduction

Transition metal silicides provided to be the promising materials for spintronics, microelectronics, and optoelectronic applications. These materials can be grown epitaxially on many different semiconductor and insulator substrates,[1–4] and its degrees of chemical and structural order can be changed by the thin film growth techniques. Their magnetic and electronic properties depend on the crystal structure and composition and vary from ferromagnetic metal (Fe_3Si[5–7]) to paramagnetic semiconductor (β-$FeSi_2$[8]).

One of the most exciting compounds from the transition metal silicides family is the Heusler compounds of T_3Si with the DO_3-type cubic crystal structure. The reason why the compound T_3Si has long attracted attention is the presence of metal properties along with high-spin polarization.[9,10] One more motivation for studying the T_3Si system (T-transition metal) is the possibility to tune its magnetic properties. The possibility of smoothly adjusting their properties by doping and temperature and switching between states under the influence of external impacts make the used as an element base for silicon-based devices. Since these impacts (e.g., pressure or doping) are associated with changes in the local environment, this stimulates us to perform detailed theoretical investigation of the effect of the local environment on the magnetic and electronic properties of T_3Si system.

Nowadays, the most studied compounds with DO3 structure from the transition metal silicides family are iron silicides. Fe_3Si is ferromagnetic metal with a high Curie temperature (≈840 K). High spin-polarization is theoretically predicted in this material,[9] so it is a potentially good candidate for a spin injector. Earlier, we investigated the effect of the local environment on the magnetic moment formation in iron silicide Fe_3Si in the framework of the suggested self-consistent approach related to the mapping of the results of the ab initio calculation on the multiorbital model.[7] It was shown that in Fe_3Si the Fe atoms have a strong sensitivity to the local environment in the second coordination sphere.

In this article, we performed the theoretical investigation of the effect of the local environment on the magnetic properties of other T_3Si Heusler compounds, namely, Mn_3Si. Unlike Fe_3Si, Mn_3Si has antiferromagnetic ordering at the Neel temperature $T_N = 23$ K with the incommensurate spin structure of a propagation vector $Q = 0.425\ G_{111}$, where G_{111} is the reciprocal lattice vector along the [111] direction.[11,12] The experimental magnetic moments on MnI and MnII atoms are $\mu_{MnI} = 2.4\ \mu_B$ and $\mu_{MnII} = -0.28\ \mu_B$ [13,14]. As was shown in previous studies,[15,16] this compound can be considered as a half-metal, and this feature is useful for the realization of spin injection through the metal-semiconductor interface. Early electronic and magnetic properties of Mn_3Si were calculated in the framework of density functional theory in previous studies.[17,18] Here, we adopt our self-consistent mapping approach for the investigation of the role of the nearest (NN) and next-nearest neighbors (NNN) in the magnetic moments formation of manganese atoms in Mn_3Si.

O. N. Draganyuk, Dr. V. S. Zhandun, Dr. N. G. Zamkova
Kirensky Institute of Physics
Federal Research Center Krasnoyarsk Science Centre
Siberian Branch of the Russian Academy of Sciences
660036 Krasnoyarsk, Russia
E-mail: jvc@iph.krasn.ru

O. N. Draganyuk, Dr. V. S. Zhandun
Reshetnev Siberian State University of Science and Technology
660037 Krasnoyarsk, Russia

The ORCID identification number(s) for the author(s) of this article can be found under https://doi.org/10.1002/pssb.201900228.

DOI: 10.1002/pssb.201900228

This article is organized as follows. In Section 2, we formulate the multiorbital model and provide the details of ab initio calculations. In Section 3, the results of the model and ab initio calculations of Mn_3Si are compared, and the dependence of magnetic moments on the hopping matrix elements is presented. The last section contains a summary of the obtained results and conclusions.

2. Calculation Methods

The complex approach developed by us to study the mechanism of the formation of the magnetic state in transition metal silicides[7] is related to studying the phase diagram of possible states in the parameter space of a multiorbital model Hamiltonian that takes into account the symmetry, the number of orbitals, and electrons of a compound of interest. To determine the stability regions of various magnetic states of the compound under study in the phase state diagram, we combined the first-principle calculation and the subsequent model analysis. As a first step, we have performed the ab initio calculation of the electronic and magnetic properties of the studied compound within the framework of density functional theory (DFT) with generalized gradient approximation (GGA). Then, self-consistent mapping of the obtained ab initio results to the model was performed.

Ab initio calculations are performed using the Vienna ab initio simulation package (VASP)[19] with projector augmented wave (PAW) pseudopotentials.[20] The valence electron configurations $3d^5 4s^2$ are taken for Mn atoms and $3s^2 3p^2$ for Si atoms. The Brillouin-zone integration is performed on the grid Monkhorst-Pack[21] special points $10 \times 10 \times 10$. Throughout all calculations, the exchange-correlation functional within the Perdew–Burke–Ernzerhoff (PBE) parameterization[22] and the plane-wave cutoff energy 500 eV were used.

The results of the ab initio calculation are mapped onto the multi-orbital model.[7] Here, we give only the Hamiltonian of the model. The detailed description of the model approach can be found in previous studies.[7,23] The model Hamiltonian is

$$H = H^{\mathrm{Mn}} + H_{J'}^{\mathrm{Mn-Mn}} + H_0^{\mathrm{Si}} + H_{\mathrm{hop}}, \quad H^{\mathrm{Mn}} = H_0^{\mathrm{Mn}} + H_{\mathrm{K}}^{\mathrm{Mn}} \tag{1}$$

where

$$H_0^{\mathrm{Mn}} = \sum \varepsilon_{0,\lambda}^{\mathrm{Mn}} \hat{n}_{n\lambda\sigma}^{d}; \quad H_0^{\mathrm{Si}} = \sum \varepsilon_{0,p}^{\mathrm{Si}} \hat{n}_{n\lambda\sigma}^{p} \tag{2}$$

the Coulomb part of the Hamiltonian

$$H_{\mathrm{K}}^{\mathrm{Mn}} = \frac{U}{2} \sum \hat{n}_{n\lambda\sigma}^{d} \hat{n}_{n\lambda\bar{\sigma}}^{d} + \left(U' - \frac{1}{2} J \right) \sum \hat{n}_{n\lambda}^{d} \hat{n}_{n\mu}^{d} (1 - \delta_{\lambda\mu}) - \frac{1}{2} J \sum \hat{s}_{n\lambda}^{d} \hat{s}_{n\mu}^{d} \tag{3}$$

The intersite exchange between nearest Mn atoms are

$$H_{J'}^{\mathrm{Mn-Mn}} = -\frac{1}{2} J' \sum \hat{s}_{n\lambda}^{d} \hat{s}_{n'\mu}^{d} \tag{4}$$

$$\mathcal{H}_{\mathrm{hop}} = \sum t_{\lambda\mu}^{nn'} \hat{n}_{n\lambda\sigma}^{\dagger} \hat{n}_{n'\mu\sigma} + Hc \tag{5}$$

where U, U', and J are the intra-atomic parameters, J' is the parameter of the intersite exchange between nearest Mn atoms. $t_{\lambda\mu}^{nn'}$ are hopping integrals between atoms Si–Si, Mn–Mn, and Mn–Si atoms. $\varepsilon_{0,\lambda}^{\mathrm{Mn}}$ and $\varepsilon_{0,p}^{\mathrm{Si}}$ are atomic levels of Mn d-electrons and Si p-electrons. All these parameters (U; U'; J, J', $t_{\lambda\mu}$, $\varepsilon_{0,t2g}^{\mathrm{Mn}}$, $\varepsilon_{0,eg}^{\mathrm{Mn}}$, $\varepsilon_{0,p}^{\mathrm{Si}}$) are fitting parameters of the model, and they are determined by the requirement that the model charge densities, obtained self-consistently, have to be as close as possible to the GGA ones. The model parameters can be found from minimization of the difference $\Delta = [\rho_{\mathrm{GGA}}(k,\sigma) - \rho_{\mathrm{model}}(k, \sigma; U; U'; J, J', t_{\lambda\mu})]^2$ between the ab initio electron density $\rho_{\mathrm{GGA}}(k, \sigma)$ and the model one $\rho_{\mathrm{model}}(k, \sigma; U; U'; J, J', t_{\lambda\mu})$ with respect to interaction parameters.[7,23] Since the Hartree–Fock equations have to be solved self-consistently for each set of the model parameters, we simplified the problem further and instead of minimization of function Δ (i.e., the differences of the model and VASP electron spin densities in each point of space), we have chosen to fit the occupation numbers of d-electrons, the magnetic moments of Mn-atoms, and partial d-densities of states for Mn atoms (see Equation (5) in the study by Zhandun et al.[23]).

3. Results and Discussion

Like the Fe_3Si compound, Mn_3Si has DO_3 type structure (Fm3m space symmetry group,[24,25] **Figure 1**) with two nonequivalent Mn atoms (MnI and MnII). The Si and MnI atoms are located at (0, 0, 0) and (1/2, 1/2, 1/2), correspondingly, while the MnII atoms occupy (1/4, 1/4, 1/4) и (3/4, 3/4, 3/4) sites. MnI and MnII atoms have different local environments. The ab initio calculated lattice parameter $a = 5.64$ Å and magnetic moments $\mu_{\mathrm{MnI}} = 2.55\,\mu_{\mathrm{B}}$ and $\mu_{\mathrm{MnII}} = -0.82\,\mu_{\mathrm{B}}$ are well agreed with experimental values $a = 5.72$ Å, $\mu_{\mathrm{MnI}} = 2.40\,\mu_{\mathrm{B}}$ and $\mu_{\mathrm{MnII}} = -0.28\,\mu_{\mathrm{B}}$.[13,14,25] The difference between experimental and ab initio magnetic moments (especially on MnII atom) arises because in theory we do not take into account the incommensurate spin structure.

In transition metal silicides with DO_3 structure, nonequivalent transition metal atoms (Fe, Mn) have different magnetic moments due to the different local environment of the corresponding atoms. MnI has eight MnII atoms as nearest neighbors (NN) and six Si atoms as next-nearest-neighbors (NNN); MnII

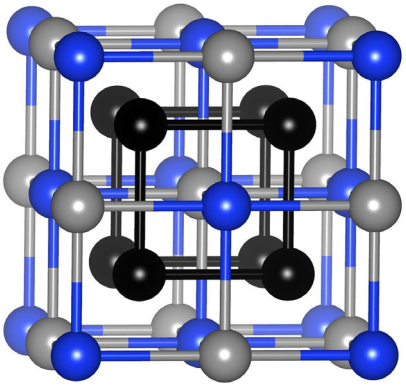

Figure 1. The Mn_3Si crystal structure. MnI, MnII, and Si atoms are shown by gray, black, and blue colors, correspondingly.

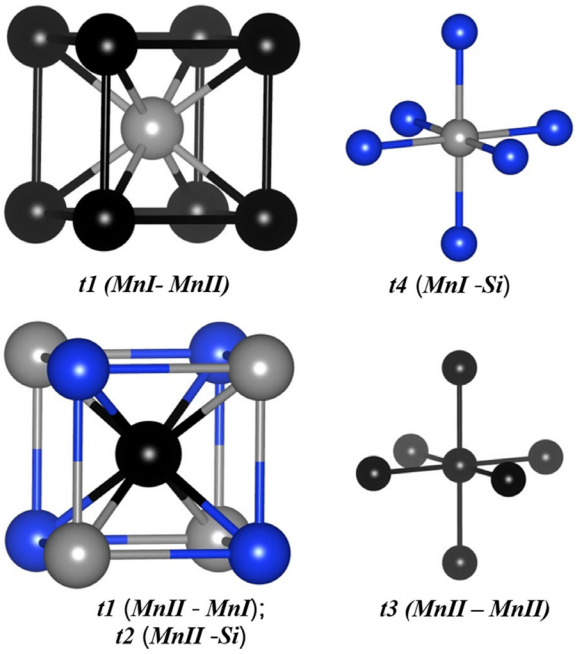

Figure 2. The local environment of MnI (gray) and MnII (black) atoms and the model hopping matrix elements in the structure of Mn_3Si. Si atoms are shown by blue balls.

has four MnI atoms and four Si atoms as NN and six MnII atoms as NNN (**Figure 2**). In the study by Zamkova et al.,[7] we have considered the effect of the local environment on the magnetic moments of iron atoms in Fe_3Si. We have found that the crucial role in the magnetic state formation is played rather by NNN Fe–Fe hoppings, than NN Fe–Si ones. Here, the role played by different hoppings in the mechanism of magnetic moments formation was analyzed in the framework of the approach described earlier (Section 2).

There are 12 hopping integrals (Figure 2): between NN Mn atoms t1 ($t1_\sigma$, $t1_\pi$, $t1_\delta$), between NN Mn and Si atoms t2 ($t2_\sigma$, $t2_\pi$), between NNN Mn atoms t3 ($t3_\sigma$, $t3_\pi$, $t3_\delta$), between NNN Mn and Si atoms t4 ($t4_\sigma$, $t4_\pi$), and between Si atoms t5 ($t5_\sigma$, $t5_\pi$). In addition, we have intra-atomic parameters (U, J, U'), atomic level energies $\varepsilon^{Si}_{0,p}$, $\varepsilon^{Mn}_{0,t2g}$, and $\varepsilon^{Mn}_{0,eg}$ and intersite exchange J' as fitting parameters in the model. The intra-atomic parameters of nonequivalent Mn atoms were equal to each other, energies of atomic levels of the nonequivalent Mn atoms were taken different due to the different local environments of MnI and MnII atoms.

The annealing method[26] was used to search for the best model parameters. The fit with such a large number of model parameters can hardly be unique and, therefore, it is sensitive to the initial configuration of magnetic moments. For this reason, we perform several testing attempts during the fitting procedure. We start the fitting procedure: 1) with the several different occupation numbers; 2) with the several different hopping parameters. Then, we have chosen the parameters that provide the best agreement according to the aforementioned criteria (occupation numbers of d-electrons, the magnetic moments of Mn-atoms, and partial d-densities of states for Mn atoms). The values of the model parameters, which provide the best fitting, are shown in **Table 1**. In **Table 2**, the comparison of DFT and model occupation numbers of Mn d-electrons ($n^d_{\lambda\sigma}$) and Mn magnetic moments (μ) are given. At this set of the model parameters, the d-orbital occupation numbers on Mn atoms in

Table 1. Model parameters (eV) providing the best fitting between model and ab initio calculations.

U	J	U'	J'	ε (Si)	ε_{t2g} (MnI)	ε_{eg} (MnI)	ε_{t2g} (MnII)	ε_{eg} (MnII)
1.67	0.45	0.80	−0.01	5.69	−0.68	0.47	−0.70	−0.50

Hopping integrals

	Nearest neighbors [NN]		Next-nearest neighbors [NNN]		
	t1 (MnI–MnII)	t2 (Mn II–Si)	t3 (MnII–MnII)	t4 (MnI–Si)	t5 (Si–Si)
σ	−1.05	0.87	0.95	0.50	0.73
π	0.30	0.59	−0.27	−0.04	0.52
δ	0.00		−0.21		

Table 2. Model and ab initio occupation numbers of the electronic d-orbitals, magnetic moments (μ), and numbers of electrons (N_{el}) of Mn atoms.

		Model				VASP			
		Occupation numbers				Occupation numbers			
Atom	Orbital	Spin up	Spin down	N_{el}	μ [μ_B]	Spin up	Spin down	N_{el}	μ [μ_B]
MnI	n_{t2g}	0.71	0.35	4.97	2.65	0.65	0.36	5.26	2.55
	n_{eg}	0.84	0.05			0.87	0.11		
MnII	n_{t2g}	0.43	0.70	5.39	−0.82	0.45	0.68	5.43	−0.82
	n_{eg}	0.49	0.51			0.42	0.44		

average deviate from the DFT ones by 3–8%. The analysis of the occupation numbers of manganese atoms in Table 2 (the model as well as ab initio) shows that large value of MnI magnetic moment is mainly determined by the MnI e_g-electrons, whereas the main contribution in the forming of MnII magnetic moment comes from the t_{2g} electrons. It is noticed that if we choose the ferromagnetic state as an initial magnetic configuration, the system still comes to the antiferromagnetic state.

The corresponding model and ab initio spin-projected partial DOSs (pDOS) of t_{2g}- and e_g-states of both Mn atoms are compared in **Figure 3**. Note that the ab initio DOSs calculated here are well agreed with other ab initio calculations.[17] Although in the model many matrix elements are neglected compared with the DFT, nevertheless, qualitatively, at this choice of parameters the model partial DOS reproduces the main features of the ab initio one (Figure 3). Similar to Fe_3Si,[7] the characteristic feature of these pDOSs is the localization of MnI d-electrons and delocalization of MnII d-electrons in the whole energy region.

To reveal the effect of NN and NNN interactions in the local environment on the Mn magnetic moment formation, we have calculated the dependence of the Mn magnetic moments on the hopping integrals $t1 \equiv t1_\sigma$ (MnI–MnII) and $t2 \equiv t2_\sigma$ (MnII–Si) in the first coordination sphere with switch on and switch off NNN hoppings ($t3 \equiv t3_\sigma$ (MnII–MnII) and $t4 \equiv t4_\sigma$ (MnI–Si)) (**Figure 4**). Since in our model the strongest type of chemical bond (σ-bond) described by hopping parameter t_σ, only this parameter was changed during all model calculations, and the ratios between t_σ, t_π, and t_δ were kept constant. The calculations were performed from two initial states: FM and AFM states. The state with minimal total energy was chosen in accordance with the Galitsky–Migdal formula.[7]

The model analysis shows that similar to the Fe_3Si, in Mn_3Si, the critical role in the mechanism of magnetism formation of MnII atom is played by the local environment in the second coordination sphere. Indeed, it is seen from Figure 4a that the switch off the NNN hoppings increases of the absolute values of MnI and MnII magnetic moments in the whole hoppings range. Wherein, the region with ab initio values of the magnetic moment is absent. This is especially true of the MnII atom for which the region with a small magnetic moment disappears and the absolute values of the magnetic moments on both MnI and MnII atoms become comparable. So, we can conclude that it is NNN hoppings that are of decisive importance in the forming of the small magnetic moments on MnII atom. The ab initio values of Mn magnetic moment appear on the phase diagram of the model only when we switch on the NNN hoppings (Figure 4b).

The further model analysis was performed to study the separate effects of metal and nonmetal environment on the magnetic moments formation. To do this, we have calculated the dependence of the magnetic moments of Mn atoms on the hopping integrals: 1) between Mn atoms (t1 and t3) and 2) between Mn and Si atoms (t2 and t4). In both cases, other hoppings integrals were fixed in according to Table 1. The calculated dependencies of the Mn magnetic moments on the hopping integrals are shown in the phase diagrams (**Figure 5** and **6**).

1) Figure 5a shows the dependence of the magnetic moments on the hopping integrals between Mn atoms in the first ($t1 \equiv t1_\sigma$) and the second ($t3 \equiv t3_\sigma$) coordination spheres. As seen, the

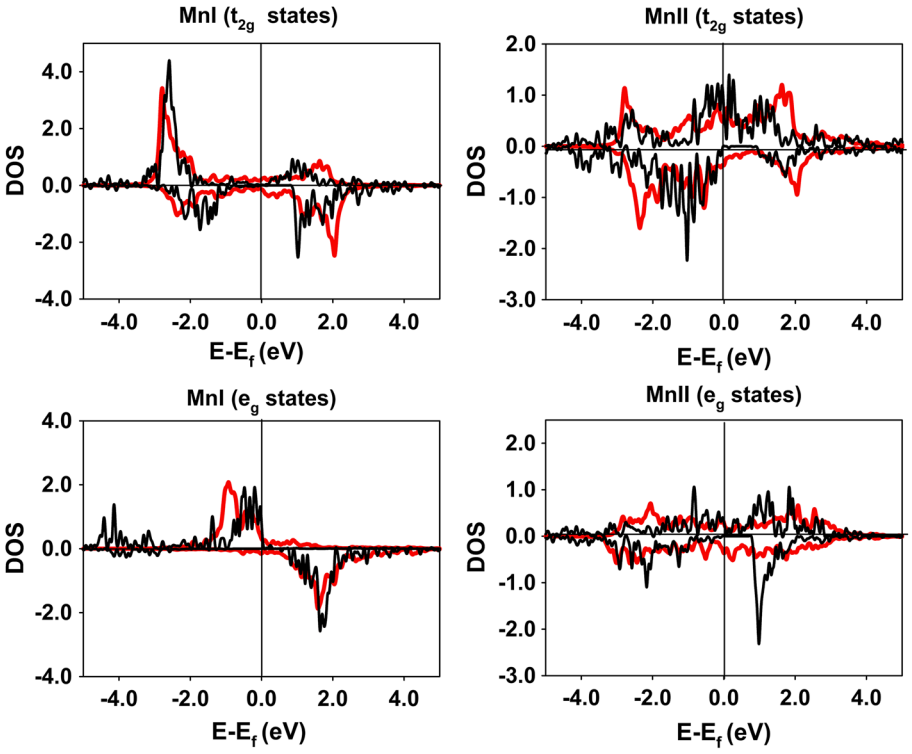

Figure 3. Comparison of the model and ab initio spin-projected partial density of d-electron states. The Fermi level is taken as the zero of energy. Positive values of DOS correspond to majority states, negative values correspond to minority states. Red lines show model DOS, black lines show ab initio DOS.

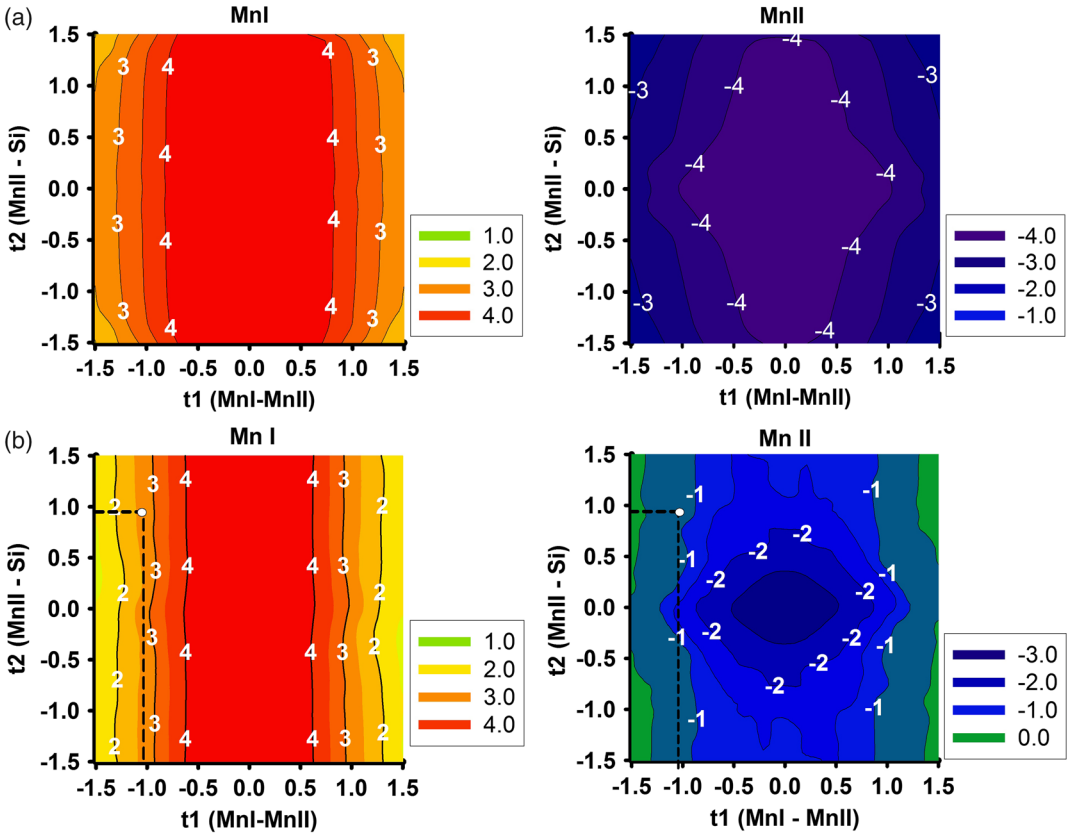

Figure 4. The model maps of the magnetic moments on MnI (left) and MnII (right) atoms in the dependence on NN hoppings: a) NNN hoppings t3 and t4 are switched off; b) NNN hoppings t3 and t4 are switched on (t3 = 0.95 eV, t4 = 0.50 eV from Table 1).

magnetic moment on MnI atom is positive and the magnetic moment of MnII atom is negative for almost whole range of hopping integrals (t1, t3). Since the environment of MnI and MnII atoms is different, these atoms have different dependence on t1 and t3 hoppings. MnI atom has Mn atoms only in the first coordination sphere, and the magnetic moment of MnI atom shows the strong dependence only on the hopping t1. The MnII atom has Mn atoms in the first as well as in the second coordination spheres; however, the change of magnetic moment of MnII atom is determined mainly by the NNN hopping t3 and practically does not depend on the hopping t1. Moreover, the magnetic moment on MnII atoms is more sensitive to the hoppings than MnI magnetic moment: the dependence of the magnetic moment of MnII atom on t3 hopping is sharper than dependence of magnetic moment of MnI atom on the hopping t1. Indeed, the magnetic moment on MnII atom decreases sharply with increase of the hopping t3 and it tends to zero at large values of hopping integral t3. This is due to the location of NNN MnII atoms along the crystallographic axes, which leads to the formation of strong σ-bonds between MnII d-electrons, and therefore, to their delocalization along the σ-bond (Figure 3, MnII d-DOS). The hopping t3 is responsible for these strong σ-bonds and play a crucial role in the decrease of the magnetic moment of MnII atom. Vice versa, MnI atom does not have manganese atoms as neighbors along the crystallographic axes and, thus, d-electrons of MnI atom remain localized and the MnI magnetic moment is large. Similar strong dependence of Fe magnetic moments on hopping integral between atoms located along the crystallographic axes was observed in the Fe_3Si compound with the same crystal structure.[7] The strong dependence of the magnetic moments of MnII atom on the hopping integral t3 results in the appearance of the sharp boundary between magnetic and nonmagnetic states of MnII atom and the ab initio magnetic state is located in instability region near this sharp boundary (Figure 5b). It should be noted that such sharp dependence of the magnetic moment on the hopping parameter t3 is characteristic not only for iron[7,23] and manganese silicides but also for nickel.[27] It can be assumed that this feature of the model phase diagrams will be preserved for other compounds with transition 3d-metals. However, if the magnetic moment on the transition metal atom is large (as, for example, in bcc-Fe $\mu \approx 2.0\,\mu_B$), then, the experimentally observed ferromagnetic state is not in the instability region (that is, near the sharp boundary between the ferromagnetic and paramagnetic phases), but in the more stable part of the phase diagram. In particular, this assumption is confirmed by the present model analysis. So, MnI atom has the large magnetic moment ($\mu \approx 2.6\,\mu_B$), and as seen from Figure 5b, its value of magnetic moment is in the more stable part and is destructed slower than the magnetic moment of MnII atom, which is $-0.8\,\mu_B$. 2) Figure 6 shows the dependence of the magnetic moments on the hopping integrals between Mn and Si atoms ($t2 \equiv t2_\sigma$ and $t4 \equiv t4_\sigma$). Since MnI atom has Si atoms

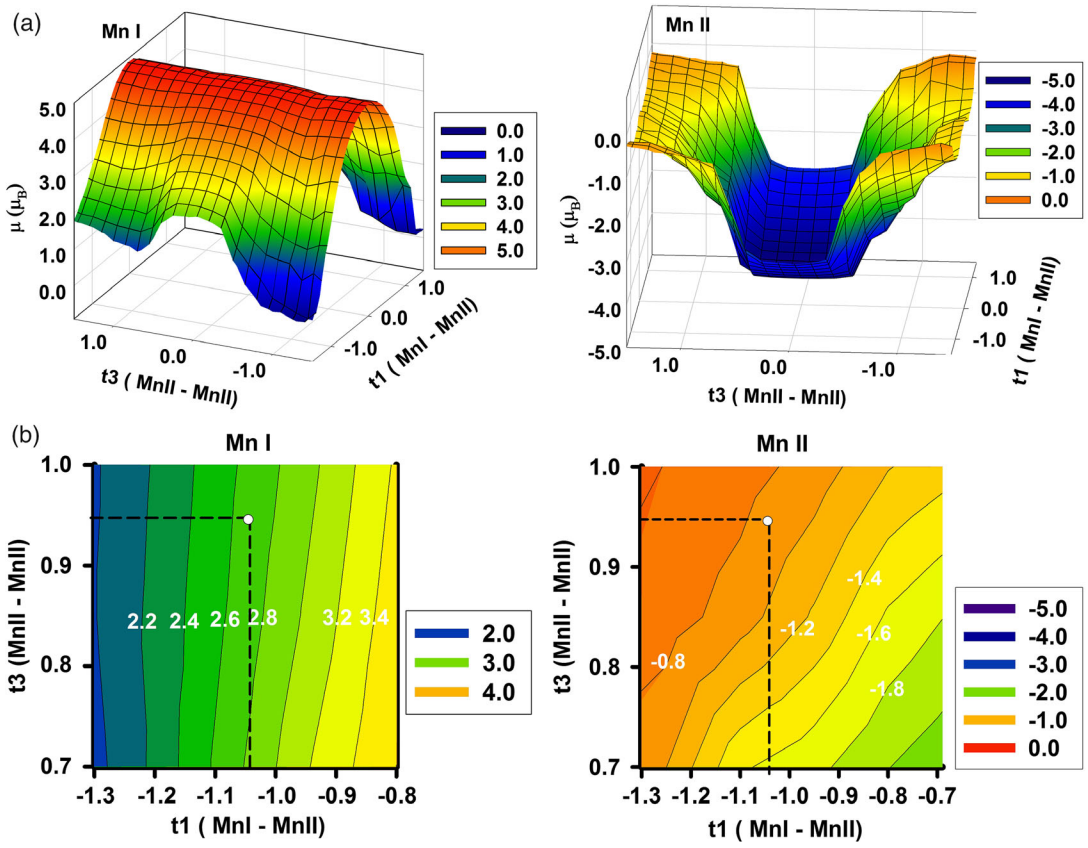

Figure 5. a) The model maps of the magnetic moments on MnI and MnII atoms in the dependence on the hoppings between Mn atoms. b) The area on the maps near the ab initio magnetic state. White point shows the hopping parameters t1 and t3 from Table 1 corresponding to the ab initio magnetic state.

only in the second coordination sphere, the magnetic moment on MnI atoms depends mainly on this hopping. However, interestingly, magnetic moments on MnII atoms depend not only on the MnII–Si hoppings t2 but also on MnI–Si hoppings t4 (Figure 6a). Although the dependence of magnetic moments on Mn–Si hoppings is too strong, however, ab initio magnetic state is located in the stable part of the phase diagram (Figure 6b) unlike (t1, t3)-phase diagram (Figure 5b). Thus, the silicon environment has minor effect on the changing of the magnetic moment.

The conclusion about the crucial role of the hopping integrals between Mn atoms and the minor role of the hopping integrals between Mn–Si atoms on the formation of the magnetic moments obtained from the model analysis was confirmed by the ab initio calculations. Following the study by Zamkova et al.,[7] we assume exponential dependence of the hopping integrals t1 and t3 on the distance $R_{\mathrm{MnI-MnII}} = \frac{a\sqrt{3}}{4}$, $R_{\mathrm{MnII-MnII}} = \frac{a}{2}$, correspondingly: $t_{1,3}(R) = B_{1,3} + A_{1,3}e^{-\gamma_{1,3}\Delta R}$, where $\Delta R = R - R_0$, R_0 is the spacing between corresponding Mn atoms ($R_0 = 2.44$ for t1, $R_0 = 2.82$ for t3) at the equilibrium lattice parameter $a_0 = 5.64$ Å; $A_{1,3}$, $B_{1,3}$, and $\gamma_{1,3}$ are fitting parameters ($A_1 = -0.29$ eV, $B_1 = -0.85$eV, $B_3 = 0.12$eV, $\gamma_1 = 4.07\text{Å}^{-1}$, $A_3 = 1.15$eV, $\gamma_3 = 1.63\text{Å}^{-1}$). The ab initio magnetic moments of MnI and MnII atoms for the different lattice parameters along with model magnetic moments are shown in **Figure 7**; the upper scale of Figure 7 shows the values of the hopping integrals t1 and t3 corresponding to the spacing $R_{\mathrm{MnI-MnII}}$ and $R_{\mathrm{MnII-MnII}}$ at the given lattice parameters. As seen, the behavior of the model and the ab initio magnetic moments are in a good agreement, despite the fact that through the model calculations the hopping integrals t2 (MnII–Si) and t4 (MnI–Si) were kept fixed according to Table 1. Remarkably, if we change only one hopping integral $t_3(R_{\mathrm{MnII-MnII}})$ (other hopping parameters t1, t2, t4 were kept fixed according to Table 1), the behavior of the model magnetic moments of MnII atom remains the same, i.e., the value of MnII magnetic moment is determined solely by the hopping integral $t_3(R_{\mathrm{MnII-MnII}})$. In turn, the behavior of MnI magnetic moment is cardinally changed: at a fixed value of $t_1(R_{\mathrm{MnI-MnII}})$ the dependence of MnI magnetic moment on hopping integral t3 becomes almost constant. This again proves that the crucial role in the magnetic moment formation of MnII and MnI atoms is played by the MnII–MnII and MnI–MnII couplings, correspondingly, while MnI–Si and MnII–Si couplings have no significant effect on the formation of the magnetic moment value at a changing lattice parameter about 10%. Thus, despite some roughness of the model, it reproduces the main feature of the magnetic moment behavior obtained in ab initio calculation, and moreover allows understanding the physical reasons of the magnetic properties of Mn_3Si in terms of the local environment.

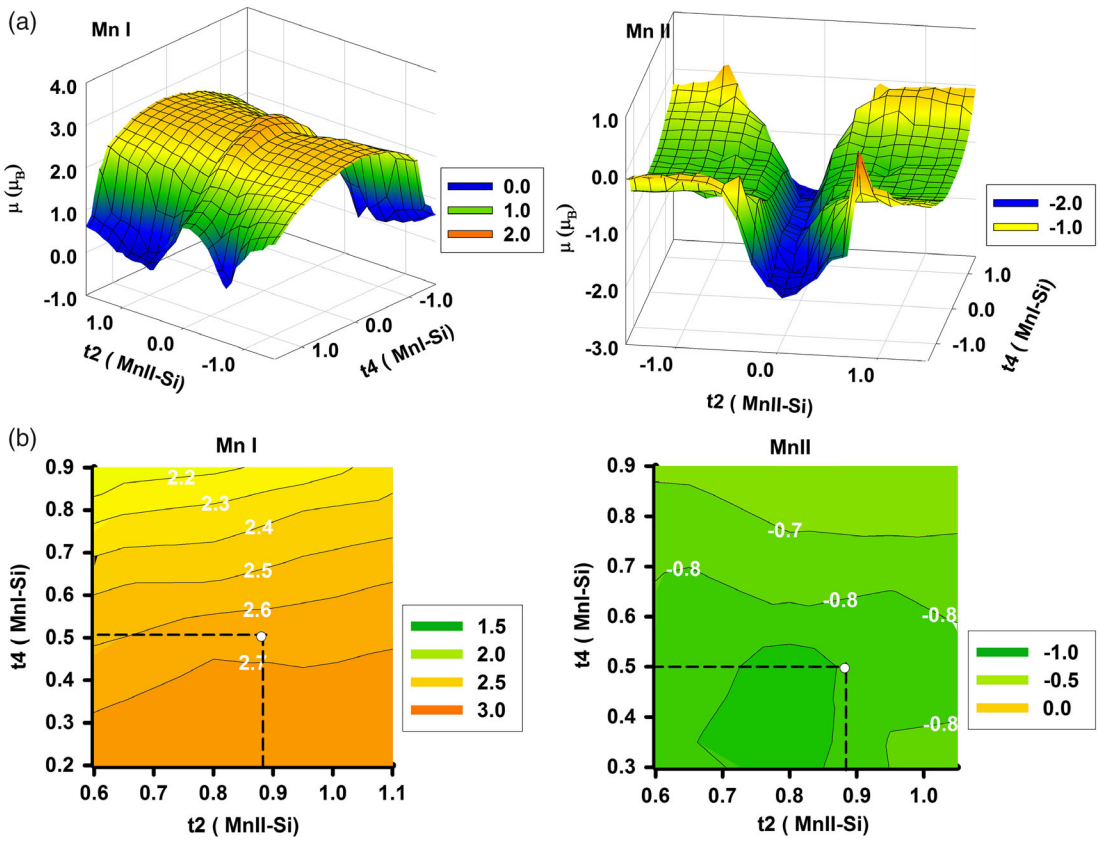

Figure 6. a) The model maps of the magnetic moments on MnI and MnII atoms in the dependence on hoppings between Mn and Si atoms. b) The area on the maps near the ab initio magnetic state. White point shows the hopping parameters t2 and t4 from Table 1 corresponding to the ab initio magnetic state.

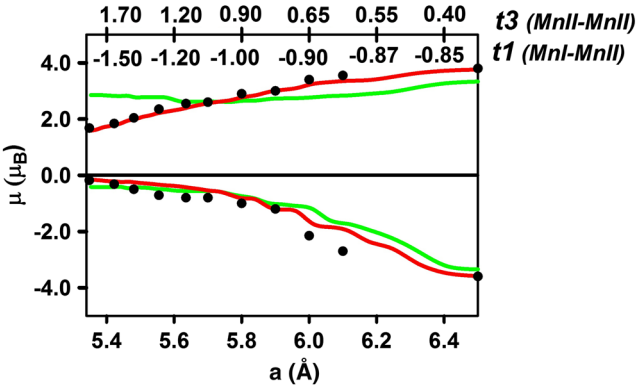

Figure 7. Black circles show the dependences of the ab initio magnetic moments on MnI and MnII atoms on the lattice parameter in calculations. Red line shows the dependence of the model magnetic moments on MnI and MnII atoms on the hopping integrals t1 (MnI–MnII) and t3 (MnII–MnII) at changing of both hopping integrals t1, t3. Green line shows the dependence of the model magnetic moments on MnI and MnII atoms on the hopping integrals t3 (MnII–MnII). Other hopping integrals are kept fixed (Table 1).

So, as follows from the model analysis, the general features of the phase diagram are 1) the manganese environment as NN as well NNN has more effect on the magnetic moment formation than the silicon environment; 2) the presence of the sharp boundary between magnetic and nonmagnetic state at the changing of the hoppings between Mn atoms (t1 or t3). It seems that the conclusion about minor role of the silicon environment in the magnetic moment formation in transition metal silicides is contradicted with the generally accepted ideas that the increase of the silicon neighbors in the nearest environment destroys the magnetic moment.[28,29] However, in contrast, the change of the number of silicon neighbors results in the change of the lattice parameter and hence the hopping integral between magnetic atoms will be also changed. Due to the presence of a sharp boundary between magnetic and nonmagnetic states, even a small change in this hopping can significantly change the magnetic moment.

Indeed, let us consider two ordered Si-rich structures of manganese silicide (**Figure 8**a,b). In the first structure, Si atoms replace MnI atoms in the DO3 structure (B2-type structure). In the second structure, Si atoms replace half of the MnII atoms in the DO3 structure. The calculated magnetic moments on Mn atoms and lattice parameters for both structures are shown in **Table 3**. In the first case, the lattice parameter slightly decreased and the magnetic moment of MnII atom disappears. Assuming the same dependence of hoppings on the distance: $t_3(R) = B_3 + A_3 e^{-\gamma_3 \Delta R}$, we obtain that this lattice parameter corresponds to hopping t3 = 1.4 eV. As can be seen from the model magnetic

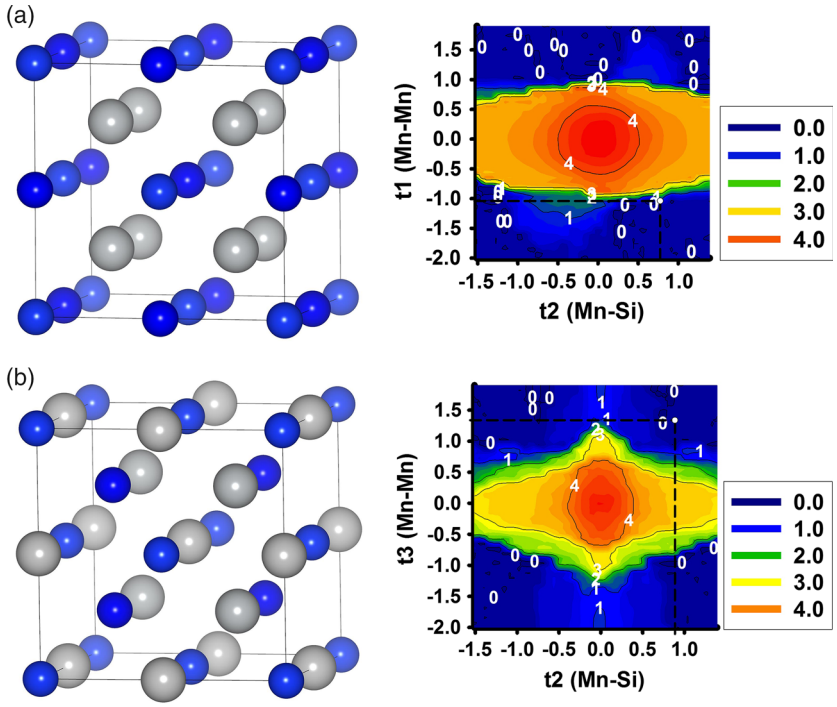

Figure 8. a) The first-ordered Si-rich structure (see text) and the map of the magnetic moments on Mn atom in the dependence on hoppings; b) the second-ordered Si-rich structure (see text) and the map of the magnetic moments on Mn atom in the dependence on hoppings.

Table 3. The lattice parameters (a) and magnetic moments (μ) of ordered Si-rich structures.

	a [Å]	μ [μ_B]
Structure No. 1	5.58	0.00
Structure No. 2	5.72	1.60

moments map of this structure (Figure 8c), even such a small change in lattice parameter gives a paramagnetic solution due to the sharp increase of the hopping t3 (MnII–MnII).

In the second case, the lattice parameter slightly increases in comparison with the initial structure and the magnetic moments of Mn atoms become equal to $\mu = 1.6\,\mu_B$. Assuming the same dependence of hoppings on the distance: $t_1(R) = B_1 + A_1 e^{-\gamma_1 \Delta R}$, we obtain that this lattice parameter corresponds to hopping $t1 = -1.1$ eV. As seen from the model magnetic moments map of this structure (Figure 8d), this value of hopping falls on the sharp boundary between the magnetic state with large magnetic moment and a paramagnetic state.

Remarkably, all obtained model phase diagrams (Figure 5, 6, and 8) show the same characteristic feature, which was mentioned earlier: a weaker dependence of magnetic moments on Mn–Si hoppings than on Mn–Mn hoppings and a sharp boundary between magnetic and paramagnetic states.

4. Conclusions

The effect of the local environment of the magnetic species on the mechanism of the magnetic state formation is well known and has long been discussed. In the present work, we studied the role played by the local environment in the moment formation in metal manganese silicide Mn_3Si. The local environment effects are studied within suggested early hybrid self-consistent mapping approach, which translates the results obtained within the DFT approach to the multiorbital model within the Hartree–Fock approximation. Model analysis makes it possible to clarify the role of NN and NNN effects of the local environment of transition metal atoms on the formation of magnetic moments.

We show that hoppings between Mn atoms control the formation of magnetism. It should be noted that not only hoppings between NN are essential for the stabilizing of the magnetic state but also NNN hoppings are important. Our model calculations show that the formation of different magnetic moments on manganese atoms is more sensitive to the values of NN and NNN hopping parameters between Mn atoms than to the Mn–Si hoppings. NN hoppings between MnI and MnII atoms have a large effect on the MnI magnetic moment formation, and NNN hoppings play a crucial role in the forming of MnII magnetic moment. The effect of the hopping between Mn and Si atoms is weaker than between Mn atoms: ab initio magnetic state is located in the stable part of the phase diagram in relation to the hoppings t2 and t4 (Mn–Si). We assume that, first of all, the effect of silicon results in the change in the lattice parameter at the change of Si concentration and only indirectly affects the magnitude of the magnetic moment through a corresponding change of hopping parameter between Mn atoms. Thus, we can conclude that, the decisive role in the formation of Mn atoms magnetic moments is played by the manganese local environment with the significant contribution of NNN hopping.

The phase diagrams of magnetic states have the characteristic features, namely, 1) the sharp boundaries between magnetic and nonmagnetic states; 2) the magnetic state of Mn_3Si is near of the sharp boundary. The presence of sharp boundary in the compounds with transition metals opens the new perspectives for practical applications of these compounds, in particular, thin films. The sharp boundary between different magnetic states is primarily related to NNN hoppings between transition metals.

In turn, NN as well as NNN hoppings are very sensitive to the change of the spacing between atoms. It means that local lattice deformations can result in significant changes in properties. The investigations of a similar effect of the local lattice deformations on the properties of materials through hoppings were performed, i.e., in previous studies.[30,31]. Therefore, various types of pressure (chemical pressure, hydrostatic pressure or depositing the films on the substrate with larger or with smaller lattice parameter) can turn on and off the magnetic state. It will stimulate experimenters to fabricate films near the magnetic-instability line with required magnetic properties.

Acknowledgements

The reported study was funded by Russian Foundation for Basic Research, Government of Krasnoyarsk Territory, Krasnoyarsk Regional Fund of Science to the research Project No. 18-42-243019: "First-principles studies of the polarization, magnetic, electronic, and magnetoelectric properties of functional compounds with a spinel structure containing 3d and 4f ions."

Conflict of Interest

The authors declare no conflict of interest.

Keywords

ab initio calculations, magnetic-instability boundaries, magnetic properties, manganese silicides, mapping, multiorbital model

Received: April 26, 2019
Revised: July 4, 2019
Published online: August 15, 2019

[1] Y. Ando, K. Hamaya, K. Kasahara K. Ueda, Y. Nozaki, T. Sadoh, Y. Maeda, K. Matsuyama, M. Miyao, *J. Appl. Phys.* **2009**, *105*, 07B102.
[2] Y. Hung, G. Y. Luo,Y. C. Chiu, P. Chang, W. C. Lee, J. G. Lin, S. F. Lee, M. Hong, J. Kwo, *Appl. Phys.* **2013**, *113*, 17C507.
[3] K. Ueda, R. Kizuka, H. Takeuchi, A. Kenjo, T. Sadoh, M. Miyao, *Thin Solid Films* **2007**, *515*, 8250.
[4] K. Tanikawa, S. Oki, S. Yamada, K. Mibu, M. Miyao, K. Hamaya, *Phys. Rev. B* **2013**, *88*, 014402.
[5] K. Ueda, T. Sadoh, Y. Ando, T. Jonishi, K. Narumi, Y. Maeda, M. Miyao, *Thin Solid Films* **2008**, *517*, 422.
[6] Y. Maeda, Y. Kawakubo, Y. Noguchi, K. Narumi, S. Sakai, *Phys. Status Solidi C* **2014**, *11*, 1570.
[7] N. G. Zamkova, V. S. Zhandun, S. G. Ovchinnikov, I. S. Sandalov, *J. Alloys Compound.* **2017**, *695*, 1213.
[8] K. Tagaya, Y. Hayashi, Y. Maeda, K. Umezawa, K. Miyake, *Jpn. J. Appl. Phys.* **2000**, *39*, 4751.
[9] A. Ionescu, C. A. F. Vaz, T. Trypiniotis, C. M. Gürtler, H. García-Miquel, J. A. C. Bland, M. E. Vickers, R. M. Dalgliesh, S. Langridge, Y. Bugoslavsky, Y. Miyoshi, L. F. Cohen, K. R. A. Ziebeck, *Phys. Rev. B* **2005**, *71*, 094401.
[10] J. Karel, J. Juraszek, J. Minar, C. Bordel, K. H. Stone, Y. N. Zhang, J. Hu, R. Q. Wu, H. Ebert, J. B. Kortright, F. Hellman, *Phys. Rev. B* **2015**, *91*, 144402.
[11] S. Tomiyoshi, E. Cowley, H. Onodera, *Phys. Rev. B* **2006**, *73*, 024416.
[12] S. Tomiyoshi, H. Watanabe, *J. Phys. Soc. Jpn.* **1975**, *39*, 295.
[13] C. Pfleiderer, J. Beouf, H. Löhneysen, *Phys. Rev. B* **2002**, *65*, 172404.
[14] H. Niki, M. Yogi, S. Nakamura, A. Uechi, S. Tomiyoshi, *Hyperfine Interact.* **2013**, *221*, 7.
[15] C. Pfleiderer, *Physica B: Condens. Matter* **2003**, *329*, 1085.
[16] M. Doerr, J. Bœuf, C. Pfleiderer, M. Rotter, N. Kozlova, D. Eckert, P. Kerschl, K.-H. Müller, M. Loewenhaupt, *Physica B: Condens. Matter* **2004**, *346–347*, 137.
[17] T. Jeong. *Physica B: Condens. Matter*, **2012**, *407*, 888.
[18] M. Hortamani, L. Sandratskii, P. Zahn, I. Mertig, *J. Appl. Phys.*, **2009**, *105*, 07E506.
[19] a) G. Kresse, J. Furthmuller, *Comput. Mater. Sci.* **1996**, *6*, 15. b) G. Kresse, J. Furthmuller, *Phys. Rev. B* **1996**, *54*, 11169.
[20] a) P. E. Blochl, *Phys. Rev. B* **1994**, *50*, 17953; b) G. Kresse, D. Joubert, *Phys. Rev. B* **1999**, *59*, 1758.
[21] H. J. Monkhorst, J. D. Pack, *Phys. Rev. B* **1976**, *13*, 5188.
[22] a) J. P. Perdew, K. Burke, M. Ernzerhof, *Phys. Rev. Lett.* **1996**, *77*, 3865; b) J. P. Perdew, K. Burke, M. Ernzerhof, *Phys. Rev. Lett.* **1997**, *78*, 1396.
[23] V. S. Zhandun, N. G. Zamkova, S. G. Ovchinnikov, I. S. Sandalov, *Phys. Rev. B* **2017**, *95*, 054429.
[24] Y. N. Babanova, F. A. Sidorenko, P. V. Gel'd, N. I. Basov, *Phys. Met. Metallogr.* **1974**, *38*, 122.
[25] B. Aronson, *Acta Chem. Scand.* **1960**, *14*, 1414.
[26] A. Khachaturyan, S. Semenovskaya, B. Vainshtein, *Acta Crystallogr. A* **1981**, *37*, 742.
[27] N. G. Zamkova, V. A. Gavrichkov, S. G. Ovchinnikov, I. S. Sandalov, *JETP Lett.* **2019**, *109*, 265.
[28] A. K. Arzhnikov, L. V. Dobysheva, E. P. Yelsukov, G. N. Konygin, E. V. Voronina, *Phys. Rev. B* **2002**, *65*, 024419.
[29] W. A. Hines, A. H. Menotti, J. I. Budnick, T. J. Burch, T. Litrenta, V. Niculescu, K. Ray, *Phys. Rev. B* **1976**, *13*, 4060.
[30] K. Sasaki, R. Saito, *Prog. Theor. Phys. Suppl.* **2008**, *176*, 253.
[31] V. Zhandun, N. Zamkova, P. Korzhavyi, I. Sandalov, *Phys. Chem. Chem. Phys.* **2019**, *21*, 13835.